ASTROBIOLOGY
Volume 9, Number 3, 2009

DOI: 10.1089/ast.2008.0255

Research Article

Monte Carlo Simulation of the Radiation Environment Encountered by a Biochip During a Space Mission to Mars

A. Le Postollec,[1,2] S. Incerti,[3] M. Dobrijevic,[1,2] L. Desorgher,[4] G. Santin,[5] P. Moretto,[3] O. Vandenabeele-Trambouze,[6] G. Coussot,[6] L. Dartnell,[7] and P. Nieminen[5]

Abstract

Simulations with a Monte Carlo tool kit have been performed to determine the radiation environment a specific device, called a biochip, would face if it were placed into a rover bound to explore Mars' surface. A biochip is a miniaturized device that can be used to detect organic molecules *in situ*. Its specific detection part is constituted of proteins whose behavior under cosmic radiation is completely unknown and must be investigated to ensure a good functioning of the device under space conditions. The aim of this study is to define particle species and energy ranges that could be relevant to investigate during experiments on irradiation beam facilities.
Several primary particles have been considered for galactic cosmic ray (GCR) and solar energetic particle (SEP) contributions. Ionizing doses accumulated in the biochip and differential fluxes of protons, alphas, neutrons, gammas, and electrons have been established for both the Earth-Mars transit and the journey at Mars' surface. Neutrons and gammas appear as dominant species on martian soil, whereas protons dominate during the interplanetary travel. Depending on solar event occurrence during the mission, an ionizing dose of around a few Grays (1 Gy = 100 rad) is expected. Key Words: Biochip—Monte Carlo simulation—Radiation—Mars—Geant4. Astrobiology 9, 311–323.

Introduction

The search for life in the Solar System is one of the great challenges of new upcoming space missions. Several techniques have been proposed to detect traces of organic matter on extraterrestrial objects. A new and promising technique based on biochips, which has been recommended by a number of space agencies, is under study internationally (Steele *et al.*, 2001; Bada *et al.*, 2005; Sims *et al.*, 2005; Parro *et al.*, 2007). A biochip is a miniaturized device composed of biological-sensitive systems, called binders, that are fixed on a solid substrate. A biochip allows for the quantification of hundreds to thousands of target molecules simultaneously (Maule *et al.*, 2005). The role of each binder is to recognize a specific molecule or family of molecules, its main characteristic being its high affinity toward an intended target. In an astrobiological context, target molecules are organic molecules, called biomarkers, that can reveal the presence of extant or extinct life. Antibodies are specific binders commonly used on biochips and could be very well adapted to detect biomarkers (Tang, 2007). Geometrically, a biochip looks like a microscope slide on which antibodies are fixed. Different kinds of material can be used for the substrate (glass, thermoplastics, elastomers), some of which may be better suited for space constraints. The biochip will allow for *in situ* analysis of a sample of extraterrestrial matter (soil, fluid, melted ice, etc.). Organic compounds contained in the sample are extracted with solvents and placed in contact with the biochip.

[1]Université Bordeaux 1, Laboratoire d'Astrophysique de Bordeaux (LAB), Floirac, France.
[2]Centre National de la Recherche Scientifique/Institut National des Sciences de l'Univers (CNRS/INSU), Floirac, France.
[3]Université Bordeaux 1, Centre National de la Recherche Scientifique/Institut National de Physique Nucléaire et de Physique des Particules (CNRS/IN2P3), Centre d'Etudes Nucléaires de Bordeaux Gradignan (CENBG), Gradignan, France.
[4]Physikalisches Institut, University of Bern, Bern, Switzerland.
[5]European Space Agency–European Space Research and Technology Centre (ESA-ESTEC), Noordwijk, the Netherlands.
[6]Institut des Biomolécules Max Mousseron (IBMM), Université Montpellier II, Montpellier, France.
[7]Centre for Mathematics and Physics in the Life Sciences and Experimental Biology (CoMPLEX), University College London, London, UK.

The detection is performed by fluorescence; if an antibody is linked to its target molecule, a fluorescent signal appears under laser excitation. This technique takes on a special interest for planetary exploration missions, as it gives a visual result of molecules present in the soil sample analyzed.

Recent missions and discoveries about Mars have come to define this planet as an advantageous target for exobiological research. *In situ* detection of organic molecules constitutes a major aim. Programs, such as the Aurora program at the European Space Agency (ESA), have begun preparation for missions that will focus on the search for traces of life on Mars. For the ExoMars mission, a biochip-based tool dedicated to the detection of molecules in soil (called a "Life Marker Chip") has been chosen as a reserve instrument.

A major concern with regard to the biochip-based instrument, however, is the reliability of this miniaturized and biological device when exposed to space conditions and, in particular, radiation hazards. Interaction of cosmic rays with the various components of the biochip must be studied to demonstrate that this kind of instrument is suitable for planetary missions. It is then imperative to conduct irradiation experiments with representative radiations in terms of nature, energy, and fluences of particles. In this context, Thompson *et al.* (2006) exposed two fluorescent dyes to low-energy proton and alpha radiation with doses that were comparable to, or in excess of, those expected during an unshielded Earth-Mars transit. They suggested that more extensive radiation testing would be needed before the suitability of these fluorophores for astrobiology missions to Mars could be fully confirmed. In particular, they noted that the shielding effect of the spacecraft creates lower-energy secondary radiation and fragments from primary radiation that might play an important role.

Indeed, during an Earth-planet transit and stay at the surface of a planet, a biochip will receive incident particles from cosmic rays and secondary particles due to the interaction of cosmic rays with the spacecraft and planetary environment (atmosphere and surface). Numerical simulations represent a valuable tool by which to define the energy spectra as well as the nature of the particles that could interact with the biochip during a typical mission. For instance, Gurtner *et al.* (2005) studied the influence of the martian atmosphere and soil in the production of secondary particles by incident galactic protons and showed that neutrons and gammas are the predominant particles at the surface for energies lower than 100 MeV.

The aim of our study was to provide a better estimation of the nature, energy, and fluences of particles that could interact with a biochip during an astrobiology mission like ExoMars. Our model takes into account the Earth-Mars transit, the shielding effect of the rover, and the interaction of galactic cosmic rays (GCR) and solar energetic particles (SEP) with the Mars environment (atmosphere and soil). A Monte Carlo code toolkit, Geant4, and some of its derived application tools, which were developed by ESA and Bern University and widely used in space simulation applications (Geant4/ESA website, 2008), were chosen to perform the simulations.

1. Materials and Method

The simulations were divided into two distinct phases: a first phase that describes the irradiation during the Earth-Mars transit and a second phase in which radiation received by the biochip at Mars' surface is modeled. As biochips perform *in situ* analysis, travel back to Earth was not considered in this study.

1.1. Geant4 simulation tool kit

Simulations were performed with the GRAS and PLANETOCOSMICS codes, both based on Geometry and Tracking 4 (Geant4).

Geant4 (Agostinelli *et al.*, 2003; Allison *et al.*, 2006) is a Monte Carlo simulation tool kit that allows the simulation of the interaction of particles with matter. It propagates elementary particles and ions through any geometrical arrangement of materials. Geant4's areas of application include: ionization, bremstrahlung, photoelectric effect, Compton scattering, elastic and inelastic hadronic interaction, nuclear capture, and particle decay. Geant4 offers different models by which to treat these physical processes. In our simulations, the electromagnetic shower was simulated by use of the standard Geant4 electromagnetic package. For the simulation of hadronic interactions, different models of Geant4 are used, depending on the energy range and primary particle type (Geant4 Physics Reference Manual, 2007). For hadrons at high energies (>10 GeV), a quark gluon string model was selected. For nucleons at energies lower than 10 GeV, the binary intranuclear cascade model was chosen. In this model, the cascade phase is followed by a pre-equilibrium phase at intermediate energy and then by an evaporation regime at lower energy. For neutrons with energy lower than 20 MeV, the G4NeutronHP model based on the ENDF database was used. For hadronic ion-ion interactions, we used the binary cascade model for light ions till 10 GeV/nuc. For higher energy, Geant4 does not provide any interaction models. Usually, one makes the approximation that the effect of an ion with N nucleons is equivalent to the effect of N protons with the same energy per nucleon. In our case, we restrained incident ion spectra to particle energies lower than 10 GeV/nuc.

Geant4 is now widely used for space applications, such as instrument design and detector response, radiation shielding, investigation of components, and biological effects. Due to its flexible object-oriented architecture and high-precision simulation capabilities, this tool offers an interesting alternative to deterministic simulation codes. Though, in use, it is still quite time consuming, Geant4 allows accurate computation that can be perfectly adapted to a special case of interest. Geant4 also offers a general-purpose simulation framework, which provides for easy interfacing with other tools and is very useful, given the large variety of application fields on irradiation issues.

1.2. Incident particles

We considered two different types of primary fluxes: GCR and SEP.

Galactic cosmic rays consist mainly of protons and ions of galactic origin that continuously and isotropically bombard our Solar System. The GCR flux in the heliosphere is modulated by the magnetic field of the solar wind and varies inversely with the 11-year solar activity cycle, which results in a GCR flux minimum during solar activity maximum and a GCR flux maximum at solar minimum. SEP events consist

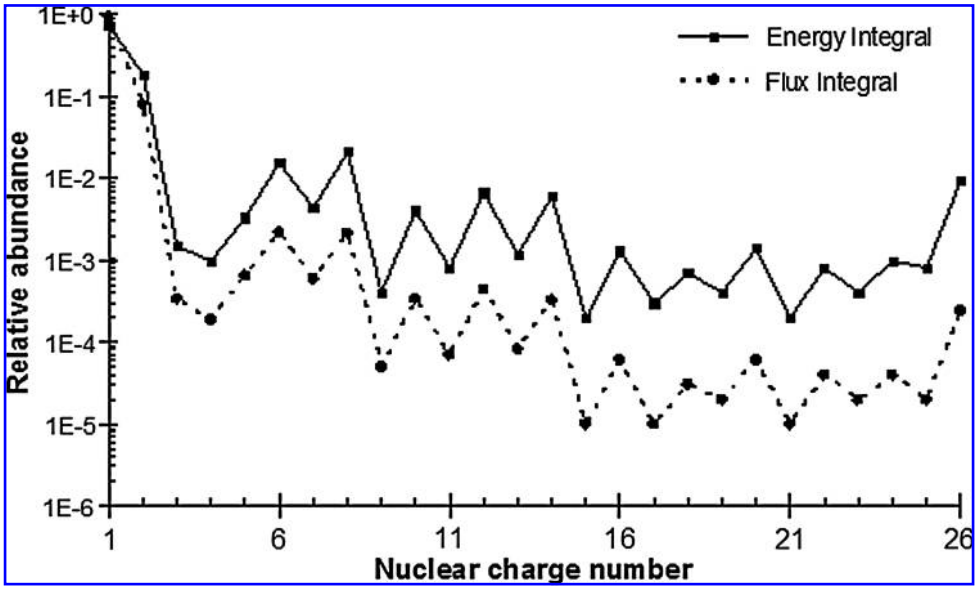

FIG. 1. Relative abundance of species from $Z=1$ to $Z=26$ in the GCR spectrum at minimum solar activity. Integral calculations are made from CREME96 spectra. They have been inspired by a similar work done by one of us (Dartnell *et al.*, 2007) who chose to model the entire GCR spectra with H, He, and C primaries.

mainly of protons that result from solar flares or coronal mass ejections. They are event driven, with occasional high fluxes over short periods (a few hours to a few days), and constitute one of the most severe environments space systems encounter. During a solar-maximum activity, the SEP events occur more frequently. Their radiation flux depends strongly on the distance between the Sun and the location of interest.

For our simulation, we chose a GCR population as described by the CREME96 model (Tylka *et al.*, 1997; High Energy Space Environment Branch, 2007, CREME96 website) for the minimum of solar activity. The considered composition of GCR is presented in Fig. 1 and is composed of ~91% protons, 8% alpha particles, and a small fraction of heavy ions dominated by carbon and oxygen ions. Only those four primary incident particles were considered in our study so as to improve upon the simulation results obtained by Gurtner *et al.* (2005), who considered only protons as primary particles. With regard to alpha particles, C and O ions, as primary particles, allowed for a more precise estimation of secondary particles produced by interaction with the biochip environment (rover, planet).

We defined the SEP population to be that which was described as the "worst week" case scenario in the CREME96 model. As CREME 96 spectra are given at 1 astronomical unit (AU), an additional scaling factor of $1/R^2$ was added to describe the dependence from the distance to the Sun [Note: for GCR, differences between spectra at Earth and Mars orbit are expected to be negligible (Webber, 1987)]. The composition of SEP in this model is illustrated in Fig. 2 and is

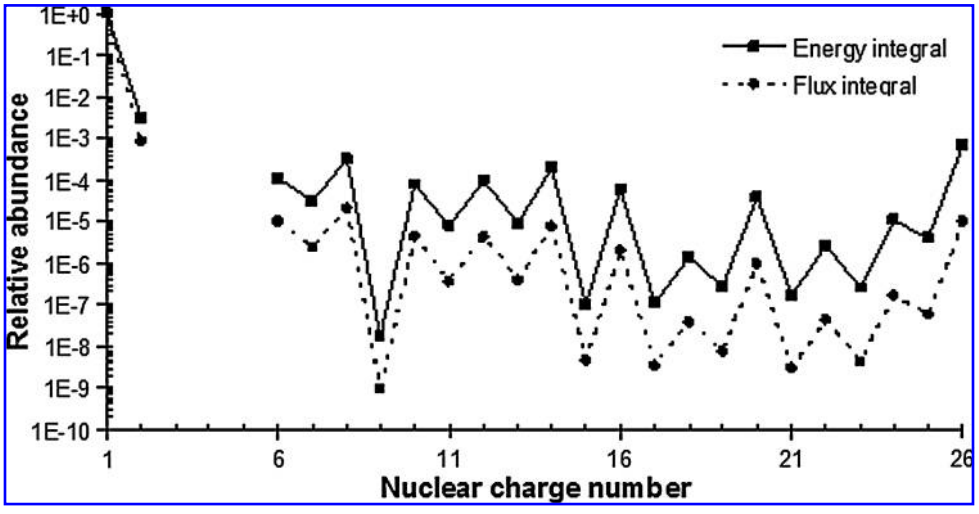

FIG. 2. Relative abundance of species from $Z=1$ to $Z=26$ in the SEP spectrum during the worst week event. Integral calculations were made from CREME96 spectra.

comprised of protons (99.9%) and few alpha particles (0.08%). SEP spectra from $Z=3$ to $Z=5$ are not available in CREME96 because those species are essentially absent from solar particle events. In the GCR, they are produced as spallation products from heavier ions (mostly oxygen and carbon) that collide with protons in the interstellar medium; but between Earth and the Sun, there are too few target nuclei for these spallation interactions to be significant. The flux of heavier ions ($Z \geq 6$) for SEP is very small, and we neglected them in our simulations.

Figure 3 summarizes the total spectrum of GCR and SEP given by the CREME96 model and considered in our simulation. It should be mentioned, however, that while the fluxes of heavier ions are indeed very low for big and heavily shielded structures (such as the International Space Station), they can be an important contributor to the overall dose via fragmentation and other secondary production. That's why we decided to consider carbon and oxygen ions for GCR, as they play an important role in ionizing dose accumulation.

1.3. Earth-Mars transit simulation with GRAS

For the transit between Earth and Mars, we simulated the interaction between cosmic particle fluxes and a simple rover model containing the biochip prototype. Primary incident spectra extracted from CREME96 interact directly with the rover. We used Geant4 Radiation Analysis in Space (GRAS) to simulate this mission phase in order to define particle fluxes and calculate ionizing doses into the biochip.

Geant4 Radiation Analysis in Space is a Geant4-based tool that deals with common radiation analysis types in 3-dimensional geometry models (Santin *et al.*, 2005). It was developed by ESA to facilitate radiation simulations in space applications and provides an interface divided into different modules by which geometries, physics models, data storing, analysis, etc., are easily defined. Analysis includes particle fluence and ionizing dose, which are of special interest in this work. GRAS uses the General Particle Source (QinetiQ, Geant4 General Particle Source website) as its generator for the primary particles, which offers many options for the choice of particle type, energy spectrum, emission point, and emission direction distribution.

Though we did not have a precise mission trajectory, the course of the spacecraft was schematized, in a first approximation, as an orbit at mid-distance between Earth and Mars (1.25 AU). Particle spectra generated by CREME96 were scaled with a $1/1.25^2$ factor for SEP events. The flux was considered to be isotropic.

We opted to implement a typical cruise duration of 180 days, during which a 7-day SEP event occurred.

A simple rover geometry definition was adopted for this travel simulation. It was a rudimentary cube (1 m^3) made of 4 mm thick aluminum that housed an aluminum box (30 cm side, 27 dm^3) at its center. The biochip, a $75\times25\times1$ mm SiO_2 slide, was positioned inside this box. The space vessel geometry was not included here. In a primary assessment of radiation effects on the instrument, we considered only the influence of a double aluminum shield provided by the rover and a dedicated biochip container, with a total thickness of 6 mm.

Primary particle fluxes were generated isotropically from a spherical source surrounding the rover (Fig. 4).

1.4. Simulation on Mars

The second phase of the mission simulation addressed irradiation received on Mars. We considered a rover exploring the surface of Mars over the course of one Earth month. In this second phase, interactions of particles with the martian atmosphere and soil added complexity to the simulation process. To simplify and clarify, a two-step strategy that used both PLANETOCOSMICS and GRAS was adopted.

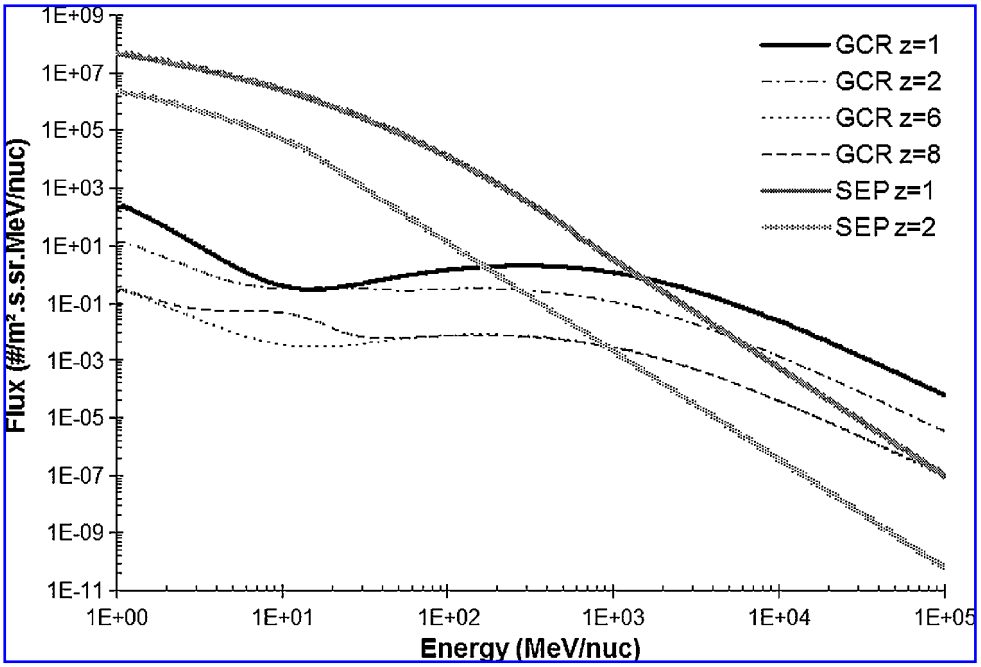

FIG. 3. Primary incident particle energy spectra extracted from CREME96 and used in this study.

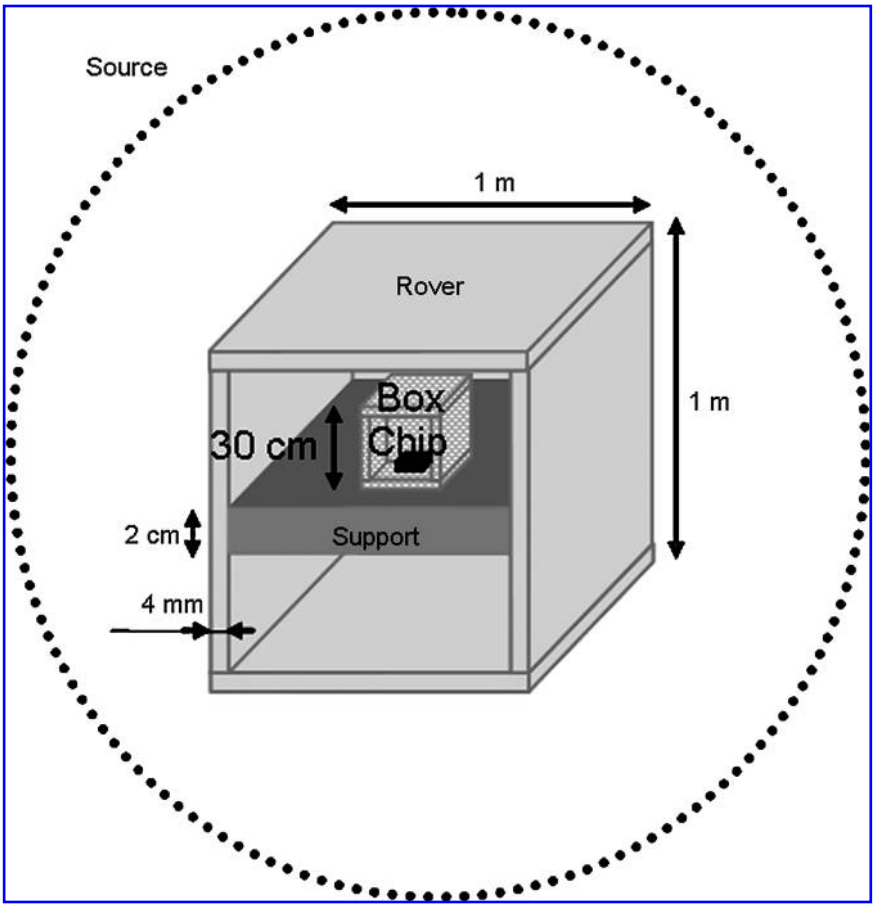

FIG. 4. Geometry implemented into GRAS simulations.

First, we investigated the particle environment the rover would encounter on Mars' surface. PLANETOCOSMICS offered the opportunity to simulate the interaction of primary particle fluxes with the martian environment.

PLANETOCOSMICS is a Geant4-based application that allows computation of electromagnetic and hadronic interactions of cosmic rays with planetary environments. For each planet, the user can simulate detailed planetary atmosphere, soil, and magnetic field (Desorgher, 2005, PLANETOCOSMICS website; Desorgher *et al.,* 2005; Bütikofer *et al.,* 2008). In our case, a martian extension of this code was used to predict the radiation level at the martian surface due to GCR and SEP events.

1.4.1. Geometry parameters. The martian environment model we constructed was basically the same as that used by Gurtner *et al.* (2005). We summarize in this section the main characteristics of this model for the atmosphere and the soil.

The martian atmosphere is very thin; the atmospheric depth varies between 8 and 22 g/cm^2 at Mars' surface. It is mainly composed of carbon dioxide, nitrogen, and argon as shown in Table 1. In PLANETOCOSMICS, the atmospheric parameters, such as density, pressure, and temperature, are provided by the 2001 Mars Global Reference Atmospheric Model (Justus *et al.,* 2006). This model uses Mars topographic information from the Mars Orbiter Laser Altimeter instrument on board Mars Global Surveyor. The program computes the atmospheric parameters versus altitude profiles as a function of position and the martian season.

Table 1. Composition of the Martian Atmosphere (Owen, 1992)

Gas	CO_2	N_2	^{40}Ar	O_2	CO	H_2O
Abundance (%)	95.32	2.7	1.6	0.13	0.07	0.03

The daily averaged atmospheric composition table of Mars at 45°N latitude and 180°E longitude (Arcadia Planitia location), on January 1, 2000, was produced for our simulations. At this position, the atmosphere was modeled by 34 layers with different thicknesses and densities, which described a 94 km thick atmosphere, from −4 km (altitude of Arcadia Planitia) to +90 km. Figure 5 shows density and surface density profiles with altitude.

The chemical composition of Mars' surface can vary greatly, especially between rock and regolith and between bright and dark dust. We chose an average martian soil composition obtained from measurements of the α-proton X-ray spectrometer on Pathfinder-Sojourner (Boyce, 2002). Abundances in different materials are given in Table 2. The soil is mainly composed of oxides, with a predominance of SiO_2.

In the simulations, the soil is defined so that the total surface thickness surpasses 1500 g/cm^2 in order to avoid

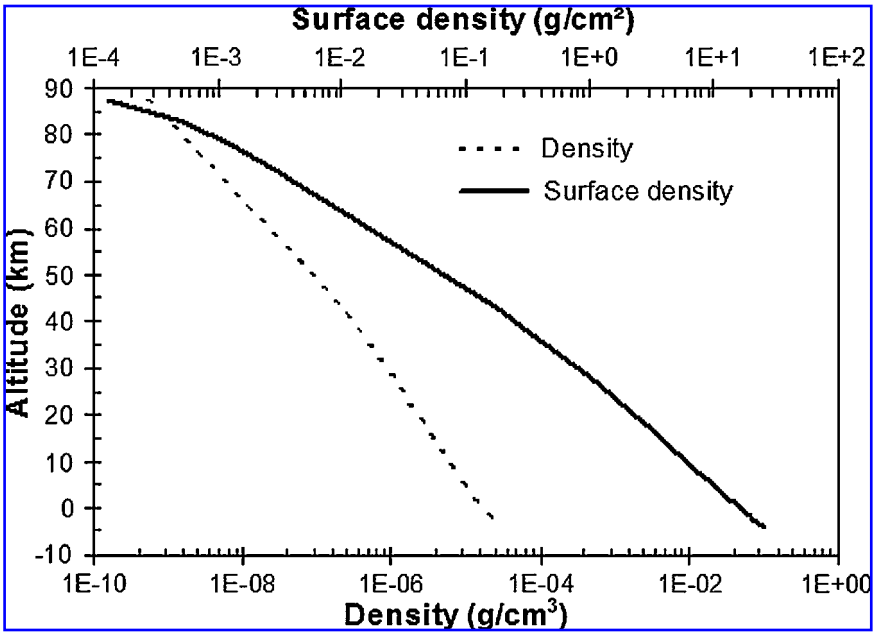

FIG. 5. Density and surface density of the daily averaged martian atmosphere as function of altitude at 45°N, 180°E. Data are provided by Mars Global Reference Atmospheric Model. (Note: the surface density corresponds to the column density integrated above the particular altitude considered.)

particle escape below the soil layer (all particles that reach the soil are stopped or backscattered). The soil density is averaged at 3.7 g/cm^3 [as in Gurtner *et al.* (2005) and Keating *et al.* (2005)], which means that the soil layer is at least 4 m thick.

The different geometry layers are defined with a sufficiently large shaped square (5000 km side, 25.10^6 km^2). The "world" of the simulation goes from 150 km above the top of the atmosphere to 10 km beyond the soil surface. A detection surface, which records upward- and downward-directed particle fluxes, is placed 1.5 m above the soil, which is the expected altitude of a biochip placed into a rover exploring the surface (see Fig. 6).

Particles are generated at the top of the world, a few kilometers above the atmosphere, from a point source. We placed a second detection surface a few meters above the top of the atmosphere to record the flux entering the atmosphere and verify whether it is identical to the flux generated for each particle type.

1.4.2. PLANETOCOSMICS/GRAS transition. Several particle fluxes above the surface are analyzed: protons, alphas, electrons, positrons, neutrons, gammas, ions from ($Z = 3$) to ($Z = 8$). Down fluxes, but also backscattered fluxes from the soil, are recorded by the detection surface. Primary particle spectra, extracted from CREME96, are scaled to 1.5 AU for SEP.

All corresponding secondary spectra on martian soil are recorded and summed up by particle type. Then, we use those results in GRAS as separate primary sources to calculate the ionizing dose received by the biochip during a 1-month stay at Mars' surface.

We developed a specific interface, based on the ROOT data analysis framework (Brun, 2008, ROOT website), to ensure compatibility of spectra produced by PLANETOCOSMICS with input spectra design expected for the GRAS simulations. While the primary incident particles injected into PLANETOCOSMICS are considered to be isotropic, the same assumption cannot be made for particles detected at rover altitude, after interaction with martian atmosphere and soil. The PLANETOCOSMICS-GRAS interface generates in GRAS primary particles on the external surface of the spherical source by taking into account the 2-dimensional energy-angle double differential distributions generated by PLANETOCOSMICS. It should be mentioned that with this interface the distribution of the primary particles over the external sphere is not considered to be uniform but is a function of the angular distribution.

Table 2. Martian Soil Composition from Alpha-Proton X-Ray Spectrometer Measurements Made by Pathfinder Sojourner (Boyce, 2002)

Material	SiO_2	Fe_2O_3	Al_2O_3	MgO	CaO	SO_3	Na_2O	TiO_2	K_2O
Abundance (%)	46.8	18.8	8.1	7.7	6.2	6	1.5	1.1	0.2

1.5. Normalization

The computation of particle fluences and deposited doses from GRAS requires a careful normalization procedure that takes into account the geometry of the simulated flux generation. The real physical quantity Q_{real}—which represents the particle fluence or the deposited dose—can be computed from

$$Q_{real} = NQ_{GRAS} \quad (1)$$

where Q_{GRAS} stands for the same physical quantity simulated with GRAS and N is a normalization factor that represents the number of particles entering the source sphere in reality. Q_{GRAS} is expressed per incident simulated event. N can be computed as the product of the section of the generation sphere around the rover multiplied by the omnidirectional impinging flux. For Earth-Mars travel, this flux is simply obtained from the energy integration of the CREME96 flux multiplied by the whole solid angle 4π. For Mars ground

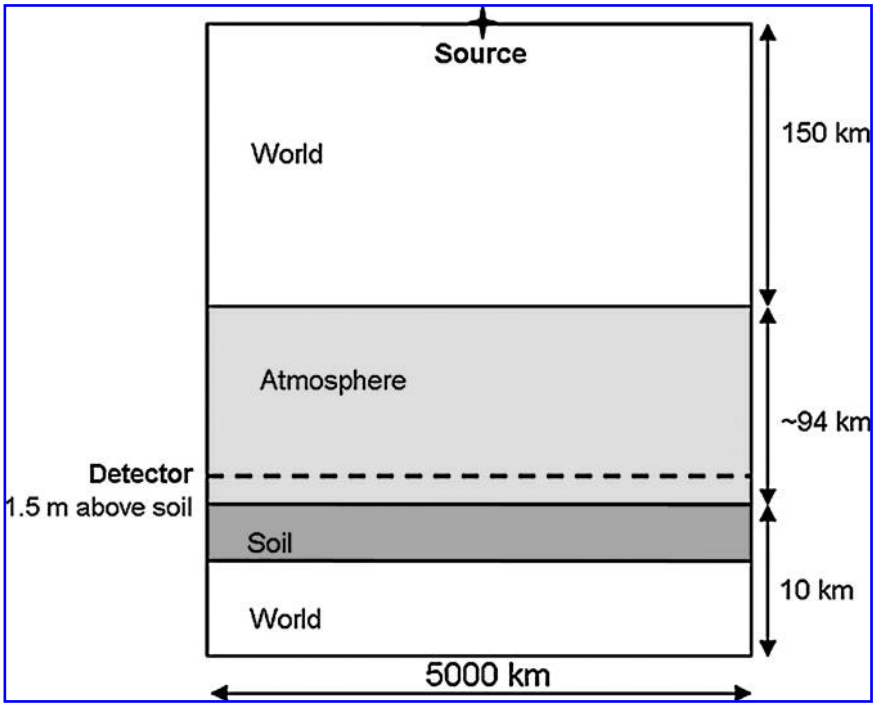

FIG. 6. Mars planetary geometry implemented into PLANETOCOSMICS simulations.

simulation, this flux is directly extracted from the PLANETOCOSMICS flux computed on the ground.

2. Results

2.1. Simulation results for Earth-Mars travel

This simulation details the interaction between the dominant particles of the cosmic spectrum and the rover geometry. Table 3 presents the amount and species of particles entering into the biochip, *i.e.*, crossing its surface, which clearly shows the creation of secondary particles when primary ones go through the rover geometry and interact with matter. Statistical errors are calculated by GRAS, following an approach very similar to the one detailed in Walters *et al.* (2002).

Differential fluxes of main particles composing the biochip environment are presented in Fig. 7. These results apply only to GCR contribution.

The different spectra highlight the effect of the rover geometry on simulations; this geometry implies modifications on the incident spectra and creates secondary particles such as neutrons, gammas, and electrons that could be of importance for the biochip's resistance and efficiency.

For ionizing dose calculations, results were divided into two parts: first the dose accumulated from GCR contribution, then the contribution of a SEP event, were considered separately. Solar proton events are unpredictable, and it seems judicious to uncouple their contribution from the GCR one.

For GCR, results per event were used to calculate global doses for a 6-month travel duration, which is typically the minimum duration required for an Earth-Mars transit. Ionizing doses in the biochip due to each type of incident primary particle of GCR spectrum are presented in Table 4. The global dose accumulated during a 6-month travel period would be on the order of 43 mGy, considering a "solar quiet" travel with only GCR contribution.

Simulations were performed with incident protons and alpha particles for the SEP contribution. As previously discussed, we considered a 7-day event with the CREME96 "worst week" model, and ionizing doses accumulated in the biochip during such an event are defined in Table 5.

Table 3. Fluxes of Particles Crossing the Biochip Surface During the Earth-Mars Travel

		Particles entering into the biochip (secondary particles)				
		Proton (p) $(\#/cm^2/s)$	*Alpha (α)* $(\#/cm^2/s)$	*Neutron* $(\#/cm^2/s)$	*Gamma* $(\#/cm^2/s)$	*Electron* $(\#/cm^2/s)$
Incident particles	p	2.17 ± 0.07	0	$(5.25 \pm 0.35)\ 10^{-1}$	1.54 ± 0.11	$(2.99 \pm 0.26)\ 10^{-1}$
	α	$(3.79 \pm 0.27)\ 10^{-2}$	$(1.61 \pm 0.04)\ 10^{-1}$	$(1.55 \pm 0.10)\ 10^{-1}$	$(3.17 \pm 0.18)\ 10^{-1}$	$(6.39 \pm 0.43)\ 10^{-2}$
	C	$(4.37 \pm 0.30)\ 10^{-3}$	$(3.61 \pm 0.39)\ 10^{-4}$	$(1.07 \pm 0.03)\ 10^{-2}$	$(2.57 \pm 0.06)\ 10^{-2}$	$(1.72 \pm 0.30)\ 10^{-2}$
	O	$(6.33 \pm 0.29)\ 10^{-3}$	$(6.43 \pm 0.62)\ 10^{-4}$	$(1.64 \pm 0.06)\ 10^{-2}$	$(4.46 \pm 0.10)\ 10^{-2}$	$(3.13 \pm 0.34)\ 10^{-2}$
Total		2.22	0.16	0.71	1.92	0.41
Total (%)		41.0%	3.0%	13.0%	35.4%	7.6%

We consider only simulations with the four dominant incident particles of the GCR spectrum. Errors are statistical errors computed by GRAS.

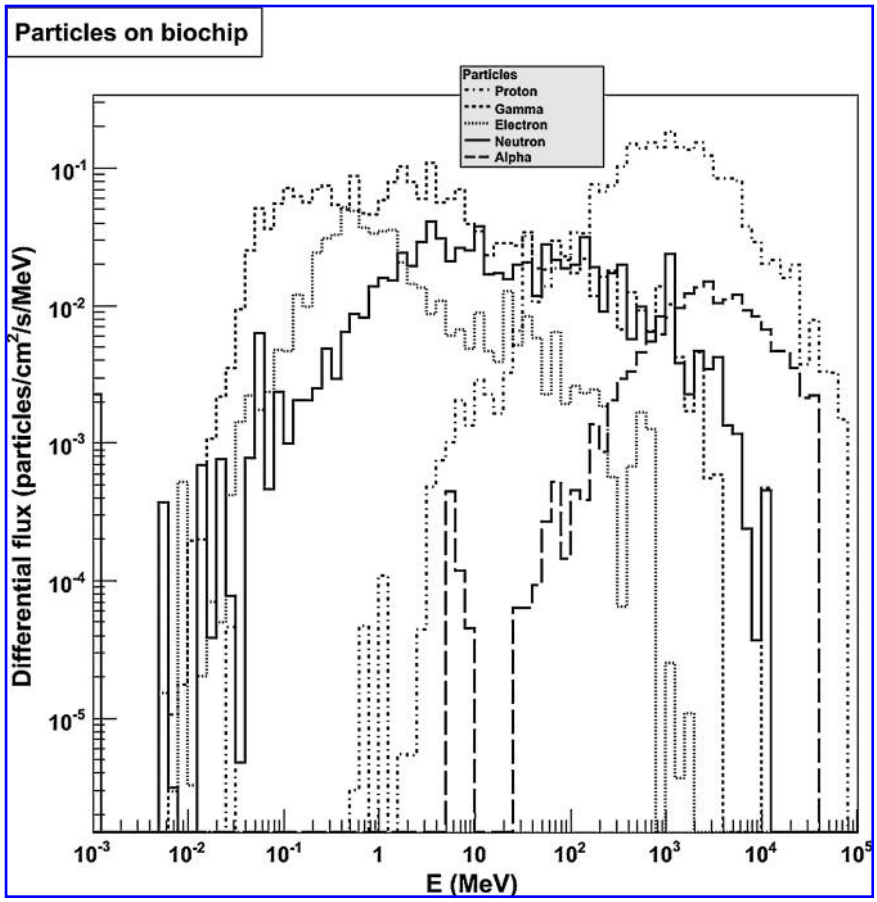

FIG. 7. Differential fluxes of protons, alphas, neutrons, gammas and electrons at biochip surface, during transit, considering GCR contribution.

The occurrence of such a big event during travel would considerably increase ionizing dose accumulation. In this case, the global ionizing dose received during the travel could reach nearly 2 Gy.

2.2. Simulation results for the stay on Mars

Simulations that had to do with martian soil reveal a large predominance of neutrons and gammas above the surface, as shown in Table 6.

Figure 8 presents differential fluxes obtained at soil level for protons, alpha particles, neutrons, gammas, and electrons, all of which reflect only GCR contribution. Figure 9 details upward and downward particle flux contributions.

We paid particular attention to neutron spectrum, with regard to future irradiation experiments on dedicated beam line facilities (*e.g.*, the AIFIRA facility of the CENBG in Bordeaux). Neutrons are produced in the atmosphere and backscattered from martian soil. The spectrum obtained at 1.5 m above the soil, with or without taking SEP into account, presents two peaks as Goldhagen *et al.* (2004) predicted. The largest one, centered on a few MeV, is due to neutron "evaporation."

The ionizing doses the biochip received during a 1-month stay at the surface of Mars were calculated with GRAS from simulations that took into account only GCR spectra (Table 7). For all GCR particle contributions, the global ionizing dose reached 27 mGy (±1 mGy).

We compared our results on Mars with predictions performed with other computing tools. De Angelis *et al.* (2006) provide the annual fluence of neutrons, protons, and ions due to GCR at the martian surface, which was simulated with the HZETRN heavy-ion code. Those results are in good agreement, in shape and order of magnitude, with the spectra presented in Fig. 8.

Radiation measurements were carried out by the Martian Environment Experiment while orbiting Mars (Zeitlin *et al.*, 2003; Saganti *et al.*, 2005) and were found to be in 10%

Table 4. Doses Received by the Biochip During a Six-Month Travel from Earth to Mars, Due to the Four Dominant Species of the GCR Spectrum

	Particles			
	Proton	*Alpha*	*Oxygen*	*Carbon*
Dose (mGy)	25.1	11.2	4.3	2.2
Statistical error (mGy)	1.28	0.37	0.13	0.06

Note: 1 Gy = 100 rad = 1 J/kg, and biochip mass = 4.4 g.

Table 5. Doses Received by the Biochip During a Seven-Day SEP Event

	Particles	
	Proton	*Alpha*
Dose (mGy)	1861.1	19.5
Statistical error (mGy)	0.4	4×10^{-4}

Table 6. Flux of Several Particles 1.5 m Above Martian Soil

Particles	*Flux without SEP (particle/cm^2/s)*	*Flux with SEP (particle/cm^2/s)*
Gamma	160.75	277.86
Neutron	80.11	145.65
Electron	8.54	11.72
Proton	5.16	15.64
Positron	2.60	2.88
Alpha	0.32	0.33
Deuteron	0.16	0.16
O	0.12	0.12
Triton	0.08	0.08
Be	0.05	0.05
C	0.05	0.05
N	0.04	0.04
Li	0.02	0.02
B	0.01	0.01
Total	258.01	454.61

Neutrons and gammas are the dominant species. (Note: SEP contribution is specifically detailed because, in this case, it is clearly overestimated, as we consider a 1-month event with the intensity of the worst-week event.)

agreement with HZETRN calculations. It will be challenging to compare these data with our model output.

Moreover, many studies on the martian radiation environment have attempted to assess biological risks for astronauts (Simonsen and Nealy, 1991; Saganti *et al.*, 2004; Cucinotta *et al.*, 2005). The high specificity of these simulations, which take body water into account for shielding and calculate increasing percentages of cancer risks, complicates any comparison with our calculations. Due to our specific scenario and our original object of interest—a biochip—our simulations are difficult to compare with others in the literature, but we emphasize that the results appear coherent with some other martian radiation predictions (Clowdsley *et al.*, 2000; Keating *et al.*, 2005; De Angelis *et al.*, 2006).

3. Conclusion and Perspectives

The simulations presented were focused on the type of particles and energy ranges a biochip would encounter during a Mars exploration mission. We defined the amount of secondary particles created during interaction with the martian environment and with the rover geometry, which were taken into consideration in our calculations of the physical quantities with regard to the ionizing dose accumulation onto the biochip.

Our developments are based on the Monte Carlo Geant4 toolkit.

Using the GRAS analysis module, we estimated with unprecedented precision the radiation environment a biochip will encounter over the course of a Mars lander mission. Abundances of protons and alpha particles around the biochip, as well as abundances of neutrons, gammas, and electrons created, were presented.

Even if the rover geometry were rudimentary, the particle environment we've defined is much more realistic than

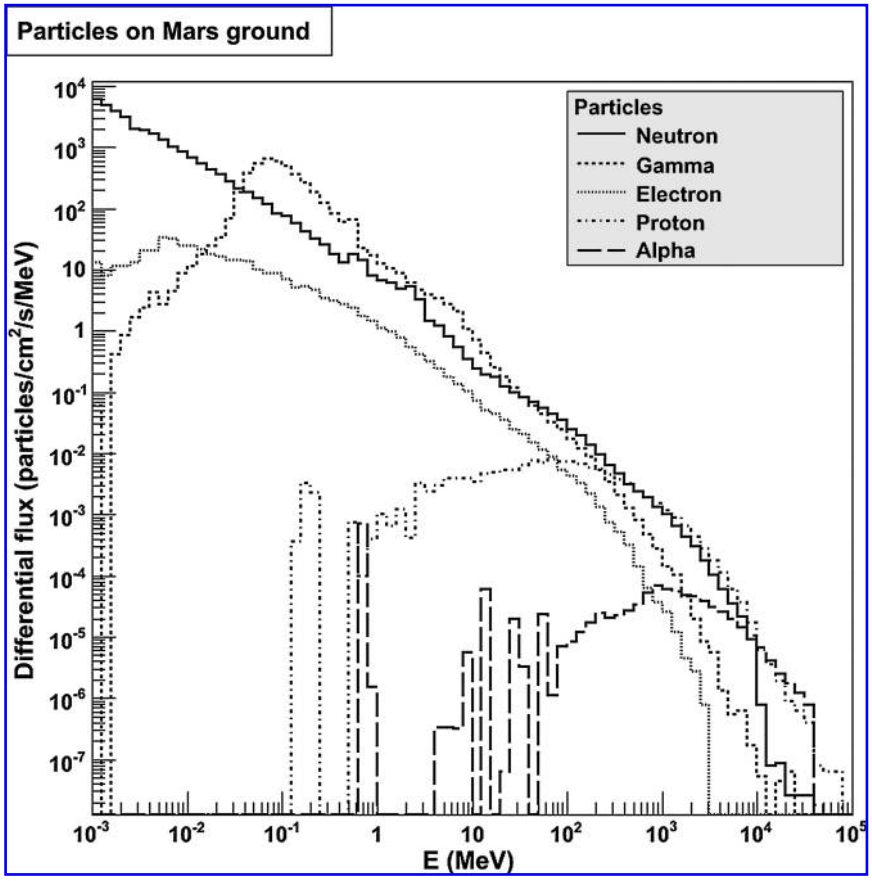

FIG. 8. Differential fluxes of protons, alphas, neutrons, gammas and electrons at 1.5 m above martian soil, obtained with PLANETOCOSMICS simulations and considering only GCR contribution.

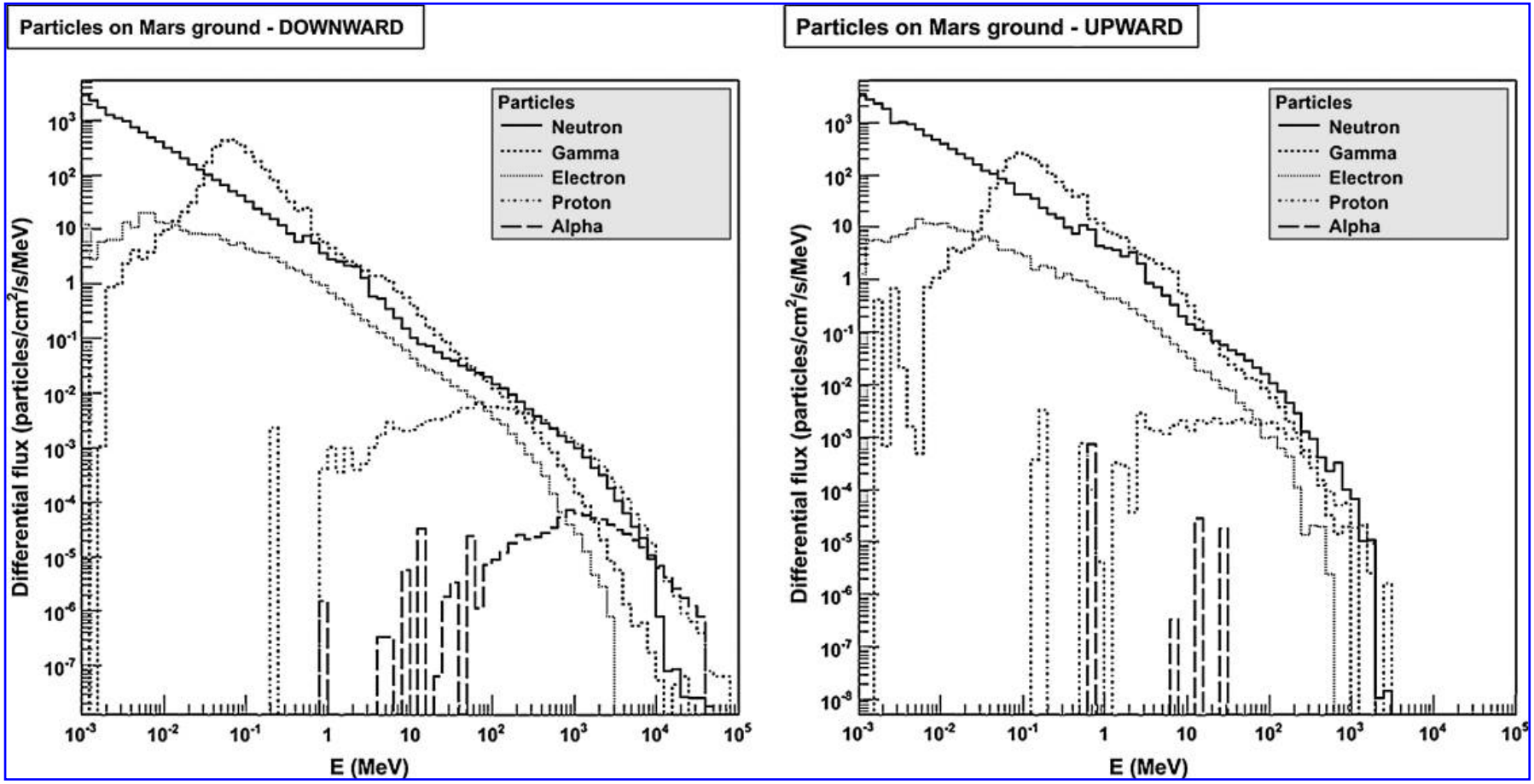

FIG. 9. Differential fluxes of upward (right) and downward (left) particles at Mars' surface, obtained with PLANETOCOSMICS.

Table 7. Doses (in mGy) Received by a Biochip During a One-Month Stay at Mars' Surface Without any SEP Event

Particles	*Dose (mGy)*	*Statistical Error (mGy)*
Proton	7.22	2.5×10^{-1}
O	7.07	3.8×10^{-1}
Gamma	1.92	3.4×10^{-1}
N	1.76	9.2×10^{-2}
Electron	1.75	8.4×10^{-2}
C	1.72	1.0×10^{-1}
Neutron	1.46	4.6×10^{-1}
Positron	1.36	4.5×10^{-2}
Alpha	1.00	2.8×10^{-2}
Be	0.84	5.4×10^{-2}
B	0.34	1.9×10^{-2}
Deuteron	0.19	8.5×10^{-3}
Li	0.16	1.1×10^{-2}
Triton	0.11	6.0×10^{-3}

traditional simulations that examine the direct interaction between incident spectra and the object of interest.

Globally, the ionizing dose received during a 6-month Mars mission, with a 7-day solar event and 1-month lander excursion, could be estimated to a few Gy. During the transit phase of the mission, protons would clearly be the most abundant species encountered and would represent the dominant contribution to the cumulative ionizing dose. At Mars' surface, interactions with the atmosphere and soil would create primarily gammas and neutrons.

This study brings an increased degree of precision to the particle environment modeling of this type of space mission; nevertheless, as solar particle events are still unpredictable, their contribution and deleterious effect remain very difficult to evaluate. Worst cases, therefore, should be considered when defining an upper limit of irradiation. A scenario with a 1-week SEP event during transit could be considered a worst case, though a realistic one as well, in that it is a good compromise between omitting or overexaggerating the solar particle contribution. Moreover, SEP fluences as a function of helioradial distance are poorly understood; hence, a geometrical scaling may not be the most appropriate treatment, given the acceleration processes taking place as the shock propagates. This is a topic of ongoing study [*e.g.,* the ESA SEPEM project (SEPEM project website)]. Therefore, it will be advantageous to refine our understanding of SEP contribution as new data on this point become available.

The ionizing dose received by the biochip during a 7-day solar event would be 2 orders of magnitude higher than the dose accumulated during a 6-month exposure to GCR. This result clearly underscores the problem posed by these energetic and unforeseeable particles.

The most abundant and the most energetic particles should be further studied, as they are both potentially harmful to a biochip. Neutrons are numerous, but their contribution to the dose would be quite low, whereas oxygen ions, for example, are few but contribute greatly to the dose accumulation.

Despite the approximations introduced in the simulations, this first estimation of doses received by a biochip during a mission to Mars allows the proposition of pertinent experimental irradiations at beam facilities. In a first step, we intend to investigate the effects of neutrons on a biochip and, in particular, on antibodies. As shielding in space devices is likely to be composed of a few millimeters of aluminum, a study dedicated to neutron effects would be of interest, even if energies involved are low, because neutrons penetrate small thicknesses of aluminum quite easily. Moreover, consequences of low-energy particles on biological systems, such as antibodies, are still unknown. Neutron irradiation on fluorescent dyes and antibodies has been performed at the Application Interdisciplinaire des Faisceaux d'Ions en Région Aquitaine (AIFIRA) facility at CENBG in Bordeaux. For these experiments, fluxes of several orders of magnitude have been used to avoid potential underestimations due to simulation inaccuracies. Indeed, even though it is continuously evolving, Geant4 faces some limitations. In particular, ion physics models are only validated for energies below 10 GeV per nucleon; therefore, we use only a reduced part of incident cosmic particle spectra in our simulations.

Description of the experimental method and preliminary results obtained from such neutron irradiation will be published soon (Le Postollec *et al.,* submitted).

Further simulations are in progress to improve the rover geometry model, considering the implementation of CAD (computer-assisted design) blueprints in Geant4. The objective is to work on shielding design and determine the best compromise between mass and protection level. Several types of materials, thicknesses, and geometries will be tested.

The possibility of including high-energy interaction models into PLANETOCOSMICS and GRAS simulations is currently under study. The use of the Particle and Heavy-Ion Transport code System (Niita *et al.,* 2007, PHITS website) could be a solution. Therefore, the energy limit of incident particles could be extended from 10 GeV/nuc up to 100 GeV/nuc.

Mars is not the only extraterrestrial body of interest for exobiological studies. Missions with astrobiological objectives to other planets or moons are under study. The same kind of simulations with new environments, such as the International Space Station (ISS) or Titan (satellite of Saturn), are under study. Simulation radiation effects on the ISS might be interesting for future experiments on board to study antibody resistance under real space constraints.

Acknowledgments

We would like to thank the French space agency (CNES), the "Région Aquitaine" and the "Institut de Physique Fondamentale" of Bordeaux (IPF) for their support.

Abbreviations

AU, astronomical units; ESA, the European Space Agency; GCR, galactic cosmic rays; Geant4, Geometry and Tracking 4; GRAS, Geant4 Radiation Analysis in Space; SEP, solar energetic particles.

References

Agostinelli, S., Allison, J., Amako, K., Apostolakis, J., Araujo, H., Arce, P., Asai, M., Axen, D., Banerjee, S., Barrand, G., Behner, F., Bellagamba, L., Boudreau, J., Broglia, L., Brunengo, A., Burkhardt, H., Chauvie, S., Chuma, J., Chytracek, R., Cooperman, G., Cosmo, G., Degtyarenko, P., Dell'Acqua, A.,

Depaola, G., Dietrich, D., Enami, R., Feliciello, A., Ferguson, C., Fesefeldt, H., Folger, G., Foppiano, F., Forti, A., Garelli, S., Giani, S., Giannitrapani, R., Gibin, D., Gomez Cadenas, J.J., Gonzalez, I., Gracia Abril, G., Greeniaus, G., Greiner, W., Grichine, V., Grossheim, A., Guatelli, S., Gumplinger, P., Hamatsu, R., Hashimoto, K., Hasui, H., Heikkinen, A., Howard, A., Ivanchenko, V., Johnson, A., Jones, F.W., Kallenbach, J., Kanay, N., Kawabata, M., Kawabata, Y., Kawaguti, M., Kelner, S., Kent, P., Kimura, A., Kodama, T., Kokoulin, R., Kossov, M., Kurashige, H., Lamanna, E., Lampen, T., Lara, V., Lefebure, V., Lei, F., Liendl, M., Lockman, W., Longo, F., Magni, S., Maire, M., Medernach, E., Minamimoto, K., Mora de Freitas, P., Morita, Y., Murakami, K., Nagamatu, M., Nartallo, R., Nieminen, P., Nishimura, T., Ohtsubo, K., Okamura, M., O'Neale, S., Oohata, Y., Paech, K., Perl, J., Pfeiffer, A., Pia, M.G., Ranjard, F., Rybin, A., Sadilov, S., Di Salvo, E., Santin, G., Sasaki, T., Savvas, N., Sawada, Y., Scherer, S., Sei, S., Sirotenko, V., Smith, D., Starkov, N., Stoecker, H., Sulkimo, J., Takahata, M., Tanaka, S., Tcherniaev, E., Safai Tehrani, E., Tropeano, M., Truscott, P., Uno, H., Urban, L., Urban, P., Verderi, M., Walkden, A., Wander, W., Weber, H., Wellisch, J.P., Wenaus, T., Williams, D.C., Wright, D., Yamada, T., Yoshida, H., and Zschiesche, D. (2003) Geant4—a simulation toolkit. *Nucl. Instrum. Methods Phys. Res. A* 506:250–303.

Allison, J., Amako, K., Apostolakis, J., Araujo, H., Arce Dubois, P., Asai, M., Barrand, G., Capra, R., Chauvie, S., Chytracek, R., Cirrone, G.A.P., Cooperman, G., Cosmo, G., Cuttone, G., Daquino, G.G., Donszelmann, M., Dressel, M., Folger, G., Foppiano, F., Generowicz, J., Grichine, V., Guatelli, S., Gumplinger, P., Heikkinen, A., Hrivnacova, I., Howard, A., Incerti, S., Ivanchenko, V., Johnson, T., Jones, F., Koi, T., Kokoulin, R., Kossov, M., Kurashige, H., Lara, V., Larsson, S., Lei, F., Link, O., Longo, F., Maire, M., Mantero, A., Mascialino, B., McLaren, I., Mendez Lorenzo, P., Minamimoto, K., Murakami, K., Nieminen, P., Pandola, L., Parlati, S., Peralta, L., Perl, J., Pfeiffer, A., Pia, M.G., Ribon, A., Rodrigues, P., Russo, G., Sadilov, S., Santin, G., Sasaki, T., Smith, D., Starkov, N., Tanaka, S., Tcherniaev, E., Tome, B., Trindade, A., Truscott, P., Urban, L., Verderi, M., Walkden, A., Wellisch, J.P., Williams, D.C., Wright, D., and Yoshida, H. (2006) Geant4 developments and applications. *IEEE Trans. Nucl. Sci.* 53:270–278.

Bada, J.L., Sephton, M.A., Ehrenfreund, P., Mathies, R.A., Skelley, A.M., Grunthaner, F.J., Zent, A.P., Quinn, R.C., Josset, J., Robert, F., Botta, O., and Glavin, D.P. (2005) New strategies to detect life on Mars. *Astronomy & Geophysics* 46:26–27.

Boyce, J.M. (2002) *The Smithsonian Book of Mars,* Smithsonian Institution Press, Washington DC, pp 77–83.

Brun, R. (2008) ROOT website. Available online at http://root.cern.ch.

Bütikofer, R., Flückiger, E.O., Desorgher, L., and Moser, M.R. (2008) The extreme solar cosmic ray influence on the radiation dose rate at aircraft altitude. *Sci. Total Environ.* 391:177–183.

Clowdsley, M.S., Wilson, J.W., Kim, M.-H.Y., Singleterry, R.C., Tripathi, R.K., Heinbockel, J.H., Badavi, F.F., and Shinn, J.L. (2000) Neutron environments on the martian surface. In *1st International Workshop on Space Radiation Research and 11th Annual NASA Space Radiation Health Investigators' Workshop,* pp 94–96.

High Energy Space Environment Branch (2007) CREME96 website. Space Science Division, Naval Research Laboratory, Washington, DC. Available online at https://creme96.nrl.navy.mil.

Cucinotta, F., Kim, M., and Ren, L. (2005) Managing lunar and Mars mission radiation risks—part I: cancer risks, uncertainties, and shielding effectiveness. *NASA Technical Paper, NASA/TP-2005-213164,* NASA, Washington, DC.

Dartnell, L.R., Desorgher, L., Ward, J.M., and Coates, A.J. (2007) Modelling the surface and subsurface martian radiation environment: implications for astrobiology. *Geophys. Res. Lett.* 34, doi: 10.1029/2006GL027494.

De Angelis, G., Wilson, J.W., Clowdsley, M.S., Qualls, G.D., and Singleterry, R.C. (2006) Modeling of the martian environment for radiation analysis. *Radiat. Meas.* 41:1097–1102.

Desorgher, L. (2005) PLANETOCOSMICS website. Available online at http://cosray.unibe.ch/~laurent/planetocosmics.

Desorgher, L., Flückiger, E.O., Gurtner, M., Moser, M.R., and Bütikofer, R. (2005) ATMOCOSMICS: a Geant4 code for computing the interaction of cosmic rays with the Earth's atmosphere. *Int. J. Mod. Phys. A* 20:6802–6804.

Geant4/ESA website. (2008) European Space Agency, ESTEC, Noordwijk, The Netherlands. Available online at http://geant4.esa.int/resources.

Geant4 Physics Reference Manual (2007) version Geant4 9.0, http://cern.ch/geant4.

Goldhagen, P., Clem, J.M., and Wilson, J.W. (2004) The energy spectrum of cosmic-ray induced neutrons measured on an airplane over a wide range of altitude and latitude. *Radiat. Prot. Dosimetry* 110:387–392.

Gurtner, M., Desorgher, L., Flückiger, E.O., and Moser, M.R. (2005) Simulation of the interaction of space radiation with the martian atmosphere and surface. *Adv. Space Res.* 36:2176–2181.

Justus, C.G., Duvall, A., and Keller, V.W. (2006) Validation of Mars Global Reference Atmospheric Model (Mars-GRAM 2001) and planned features. *Adv. Space Res.* 38:2633–2638.

Keating, A., Mohammadzadeh, A., Nieminen, P., Maia, D., Coutinho, S., Evans, H., Pimenta, M., Huot, J.-P., and Daly, E. (2005) A model for radiation environment characterization. *IEEE Trans. Nucl. Sci.* 52:2287–2293

Le Postollec, A., Coussot, G., Baqué, M., Incerti, S., Desvignes, I., Moretto, P., Dobrijevic, M., and Vandenabeele-Trambouze, O. Investigation of neutron radiation effects on antibodies and fluorescent dyes dedicated to astrobiology applications. *Astrobiology,* submitted.

Maule, J., Toporski, J., Wainwright, N., and Steele, A. (2005) An integrated system for labeling and detection of biological molecules in Mars analog regolith using an antibody microarray [abstract 1921]. In *36th Lunar and Planetary Science Conference Abstracts,* Lunar and Planetary Institute, Houston.

Niita, K., Iwase, H., Sato, T., Iwamoto, Y., Matsuda, N., Sakamoto, Y., Nakashima, H., Mancusi, D., and Sihver, L. (2007) PHITS website. Japan Atomic Energy Agency, Ibaraki Prefecture (Tokaimura), Japan. Available online at http://rcwww.kek.jp/research/shield/phits.html.

Owen, T. (1992) The composition and early history of the atmosphere of Mars. In *Mars,* edited by H.H. Kieffer, B.M. Jakosky, C.W. Synder, and M.S. Matthews, The University of Arizona Press, Tucson, AZ, pp 818–834.

Parro, V., Rivas, L.A., and Gómez-Elvira, J. (2007) Protein microarrays-based strategies for life detection in astrobiology. *Space Sci. Rev.* 135:293–311.

QinetiQ, Geant4 General Particle Source website. Available online at http://reat.space.qinetiq.com/gps.

Saganti, P., Cucinotta, F., Wilson, J., Simonsen, L., and Zeitlin, C. (2004) Radiation climate for analyzing risks to astronauts on the Mars surface from galactic cosmic rays. *Space Sci. Rev.* 110:143–156.

Saganti, P., Cucinotta, F., Cleghorn, T., Zeitlin, C., Lee, K., Hu, X., Pinsky, L., Anderson, V., Riman, F., Flanders, J., Atwell, W.,

and Turner, R. (2005) MARIE measurements and model predictions of solar modulation of galactic cosmic rays at Mars. In *29th International Cosmic Ray Conference* 1:319–322.

Santin, G., Ivanchenko, V., Evans, H., Nieminen, P., and Daly, E. (2005) GRAS: A general-purpose 3-D modular simulation tool for space environment effects analysis. *IEEE Trans. Nucl. Sci.* 52:2294–2299.

SEPEM project website. Available online at http://www.oma.be/SEPEM.

Simonsen, L. and Nealy, J., (1991) Radiation protection for human missions to the Moon and Mars. *NASA Technical Paper 3079,* NASA, Washington, DC.

Sims, M.R., Cullen, D.C., Bannister, N.P., Grant, W.D., Henry, O., Jones, R., McKnight, D., Thompson, D.P., and Wilson, P.K. (2005) The specific molecular identification of life experiment (SMILE). *Planet. Space Sci.* 53:781–791.

Steele, A., McKay, D., Allen, C., Thomas-Keprta, K., Warmflash, D., Pincus, S., Schweitzer, M., Priscu, J., Sears, J., Hedgecock, J., Avci, R., and Fogel, M. (2001) Mars Immunoassay Life Detection Instrument for astrobiology (MILDI) [abstract 1684]. In *32nd Lunar and Planetary Science Conference Abstracts,* Lunar and Planetary Institute, Houston.

Tang, B.L. (2007) A case for immunological approaches in detection and investigation of alien life. *Int. J. Astrobiology* 6:11–17.

Thompson, D.P., Wilson, P.K., Sims, M.R., Cullen, D.C., Holt, J.M.C., Parker, D.J., and Smith, M.D. (2006) Preliminary investigation of proton and helium ion radiation effects on fluorescent dyes for use in astrobiology applications. *Anal. Chem.* 78:2738–2743.

Tylka, A.J., Adams, J.H., Boberg, P.R., Brownstein, B., Dietrich, W.F., Flueckiger, E.O., Petersen, E.L., Shea, M.A., Smart, D.F., and Smith, E.C. (1997) CREME96: a revision of the Cosmic Ray Effects on Micro-Electronics Code. *IEEE Trans. Nucl. Sci.* 44:2150–2160.

Walters, B.R.B., Kawrakow, I., and Rogers, D.W.O. (2002) History by history statistical estimators. *Med. Phys.* 29:2745–2752.

Webber, W.R. (1987) The interstellar cosmic ray spectrum and energy density. Interplanetary cosmic ray gradients and a new estimate of the boundary of the heliosphere. *Astron. Astrophys.* 179:277–284.

Zeitlin, C., Cleghorn, T., Cucinotta, F., Saganti, P., Andersen, V., Lee, K., Pinsky, L., Atwell, W., and Turner, R. (2003) Results from the martian radiation environment experiment MARIE [abstract 1878]. In *34th Lunar and Planetary Science Conference Abstracts,* Lunar and Planetary Institute, Houston.

Address reprint requests to:
Aurélie Le Postollec
Laboratoire d'Astrophysique de Bordeaux
2 rue de l'Observatoire
33270 Floirac
France

E-mail: lepostollec@obs.u-bordeaux1.fr
lepostol@cenbg.in2p3.fr

This article has been cited by:

1. A. Le Postollec , G. Coussot , M. Baqué , S. Incerti , I. Desvignes , P. Moretto , M. Dobrijevic , O. Vandenabeele-Trambouze . 2009. Investigation of Neutron Radiation Effects on Polyclonal Antibodies (IgG) and Fluorescein Dye for Astrobiological ApplicationsInvestigation of Neutron Radiation Effects on Polyclonal Antibodies (IgG) and Fluorescein Dye for Astrobiological Applications. *Astrobiology* **9**:7, 637-645. [Abstract] [PDF] [PDF Plus]